

# Articulation kinematics and modeling of larynx, vocal tract and face

Jorge C. Lucero

Dept. Mathematics – Univ. Brasilia

SPSASSD - São Paulo, 7-11 June 2010

# Part I

## Physical models of the vocal folds

# Introduction

## Physical model

- Mathematical representation of the physical principles of phonation.
- It allows us to understand underlying mechanisms and simulate its behavior by computers (what happens if...) in normal and abnormal configurations.
- Applications: methods and computer tools for clinical diagnosis, voice and speech synthesis, man-machine interfaces, etc.

## Collaborations

Laura L. Koenig, Haskins Labs and Long Island University (USA)  
Xavier Pelorson, Gipsa Lab/CNRS

## Some facts

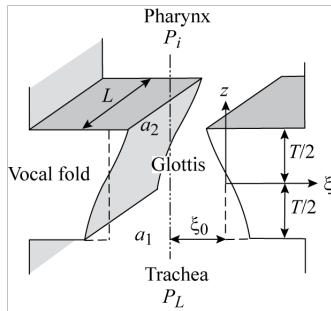
- The vocal fold oscillation is induced by the airflow through the glottis.
- It modulates the airflow, producing an acoustic wave which is injected into the vocal tract (source-filter theory).
- The same aeroelastic phenomenon also produces sound at the syrinx in songbirds, in blood arteries during sphygmomanometry, at the lips when playing a brass musical instrument, at the nostrils when blowing the nose, at the soft palate when snoring.
- Physical models: since Van den Berg (1957) experimental studies on glottal aerodynamics.
- Low-dimensional models: they are simple and allow for a better understanding of the oscillation dynamics, at the same time they capture complex nonlinear phenomena.

# Structure

Three interconnected blocks:

- ① Biomechanical structure of vocal fold tissues.
- ② Aerodynamics of glottal flow.
- ③ Propagation of acoustical wave on the vocal tract.

## Tissue motion



A surface wave propagates through the tissues in the direction of the airflow (Titze, 1988).

From the wave equation

$$\frac{\partial^2 \xi}{\partial t^2} = c^2 \frac{\partial^2 \xi}{\partial z^2}$$

we obtain

$$\begin{aligned} a_1(t) &= 2L[\xi_0 + \xi(t + \tau)] \\ &\approx 2L[\xi_0 + \tau \dot{\xi}(t)] \end{aligned}$$

$$\begin{aligned} a_2(t) &= 2L[\xi_0 + \xi(t - \tau)] \\ &\approx 2L[\xi_0 - \tau \dot{\xi}(t)] \end{aligned}$$

## Biomechanics

All biomechanics is lumped at the midpoint

$$M\ddot{\xi} + h(\xi, \dot{\xi}) + K\xi = P_g$$

$P_g$  is the mean glottal air pressure, and  $h(\xi, \dot{\xi})$  is related to the energy dissipated in the tissues

$$h(\xi, \dot{\xi}) = B\dot{\xi} \quad (\text{Titze, 1988})$$

or, even better

$$h(\xi, \dot{\xi}) = B\dot{\xi} + C\xi^2\dot{\xi} \quad (\text{Laje et al., 2001})$$

$C\xi^2\dot{\xi}$  represents the effect of vocal fold collision, nonlinear characteristics of tissues, and any other nonlinear phenomena. It introduces a saturation effect at large oscillation amplitudes.

## Glottal aerodynamics

Bernoulli flow up to the glottal exit, therefore:

$$P_s = P_2 + k_t \frac{\rho}{2} \frac{u_g^2}{a_2^2}$$

$P_s$  is the subglottal pressure and  $u_g$  the air flow.

At the glottal exit, all flow energy is lost to turbulence

$$P_2 = P_i$$

The mean glottal air pressure is

$$P_g = \frac{1}{T} \int_{-T/2}^{T/2} P(z) dz = P_i + \frac{P_s - P_i}{k_t} \left( 1 - \frac{a_2}{a_1} \right)$$

## Oscillation mechanism

- If  $\tau$  is small enough and  $P_i = 0$ ,

$$P_g \approx \frac{2P_s\tau\dot{\xi}}{\xi_0 + \xi}$$

- Glottis opening:  $\dot{\xi} > 0 \implies a_1 > a_2 \implies P_g > 0$
- Glottis closing:  $\dot{\xi} < 0 \implies a_1 < a_2 \implies P_g < 0$
- For small  $\xi$ ,  $P_g \approx \alpha P_s \dot{\xi}$ , and the equation of motion is

$$M\ddot{\xi} - (\alpha P_s - B - C\xi^2)\dot{\xi} + K\xi = 0$$

which has the form of the relaxation oscillator (Van der Pol equation)

$$\ddot{\xi} - \mu(1 - \xi^2)\dot{\xi} + \xi = 0$$

## Phonation threshold pressure

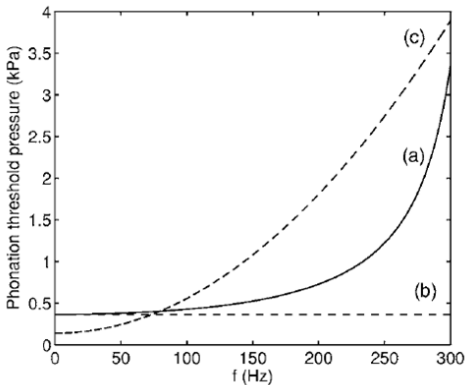
$$P_{\text{th}} = \frac{k_t \xi_0 B \omega}{2 \sin(\omega \tau)}$$

(Lucero and Koenig, 2007)

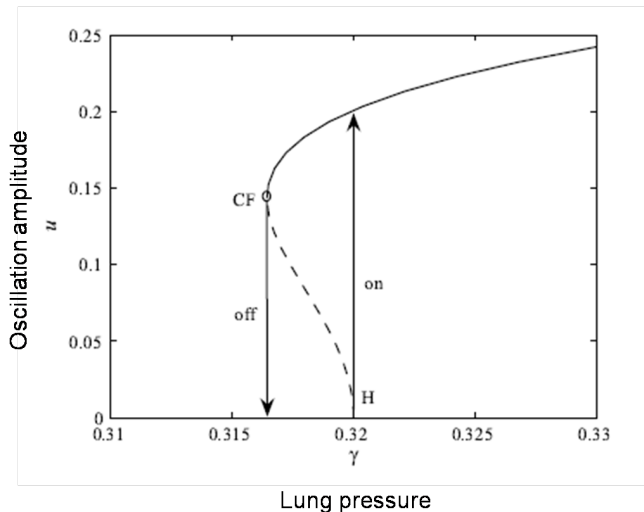
and, if  $\tau$  is very small,

$$P_{\text{th}} = \frac{k_t \xi_0 B}{2 \tau}$$

(Titze, 1988).



## Oscillation hysteresis



Oscillation onset is a subcritical Hopf bifurcation (Lucero, 1999).

## Phonation onset-offset hysteresis

- Excised larynges (Baer, 1981; Berry et al., 1995) and physical models (Titze et al., 1995; Ruty et al., 2007): the subglottal pressure is lower at oscillation offset than at oscillation onset.
- In speech, intraoral pressure is lower at voice onset compared to voice offset (Munhall et al., 1994), the airflow is lower (Lucero and Koenig, 2005), the transglottal pressures is higher (Hirose and Niimi, 1987), and the glottal width is smaller (Hirose and Niimi, 1987).
- The vocal fold configuration at oscillation onset seems to be always more restricted than the configuration at offset, or,
- it is easier to maintain voice after it has started.

## Size influence

- Scale factor  $\beta = 1$  adult man, 0.72 adult woman, 0.64 5-year-old child.
  - Dimensions  $d = \beta d_{\text{man}}$ .
  - Mass  $M = \beta^3 M_{\text{man}}$ .
  - The modulus of elasticity and damping coefficient of tissues are constant.
- Phonation threshold pressure

$$P_{\text{th}} = \frac{k_t \xi_0 B \omega}{2\beta \sin(\delta)} \quad \delta = \omega \tau$$

- Smaller larynges demand a larger phonation threshold pressure. The vocal fold surface is smaller, and absorb less energy from the airflow.

## Threshold vs. size

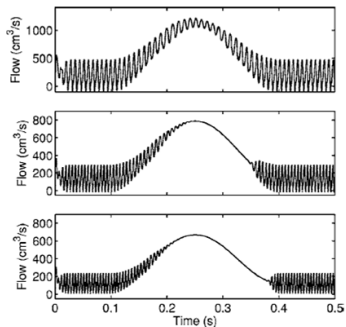


FIG. 2. Oral airflow patterns during a vocal fold abduction-adduction gesture. Top panel:  $\beta=1$  (male adult), middle: panel  $\beta=0.72$  (female adult), bottom panel:  $\beta=0.64$  (5-year-old child).

(Lucero and Koenig,2005)

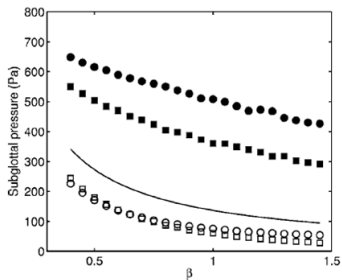


FIG. 4. Oscillation thresholds of subglottal pressure. Circles: thresholds when using the full equations of the model; squares: thresholds when neglecting the effects of air viscosity and the vocal tract. In both cases, the closed marks indicate the oscillation onset, and the open marks indicate the offset. Full line: value predicted by Eq. (5).

## Vocal tract

- When the oscillation frequency ( $F_0$ ) is well below the first formant ( $F_1$ ), the vocal tract is an inertive load

$$P_i \approx l \dot{u}_g \quad l = \rho l / A$$

$l$  is the vocal tract length and  $A$  is its cross-sectional area.

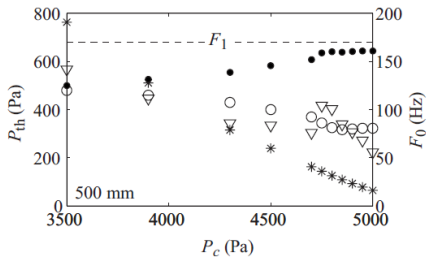
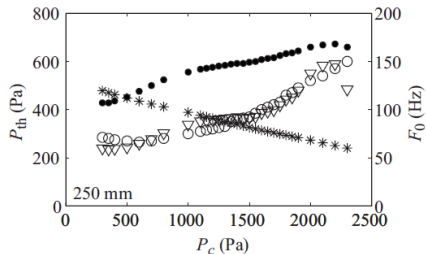
- The threshold pressure is

$$P_{\text{th}} = \frac{k_t \xi_0 B \omega}{2 \sin(\omega \tau)} - k_t \xi_0 L l v_2 \omega \cot(\omega \tau)$$

(Lucero et al., 2009)

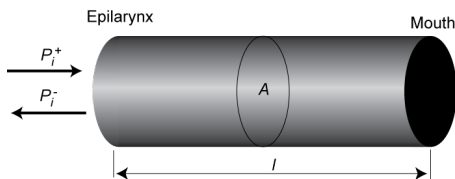
- The vocal tract lowers the threshold pressure

## Threshold pressure



Circles: data from a mechanical replica (Ruty et al., 2007)  
Stars: Titze's model (1988)  
Triangles: Extended model  
Full circles:  $F_0$

# Acoustical wave propagation



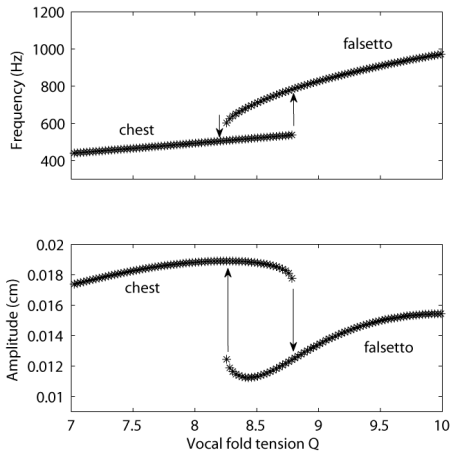
$$\begin{aligned}P_i(t) &= P_i^+(t) + P_i^-(t) \\ &= P_i^+(t) + rP_i^+(t - \nu) \\ &= \alpha\sqrt{P_s}[x(t) + rx(t - \nu)]\end{aligned}$$

where

$$\alpha = \frac{2l\rho c}{A} \sqrt{\frac{2}{\rho k_t}} \quad (\text{coupling coefficient})$$

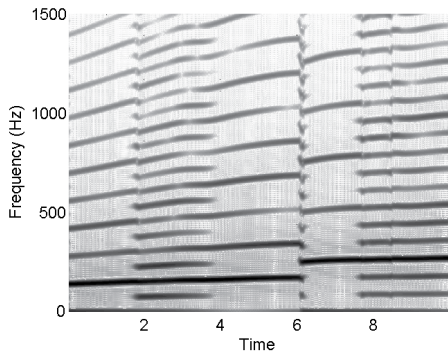
(Arneodo and Mindlin, 2009)

## Chest-falsetto



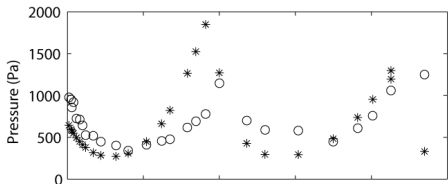
$F_1 = 500$  Hz  
Frequency and amplitude  
jumps when  $F_0 = F_1$ .

## Singing into a tube



Singing: increasing  $F_0$ .  
 $F_1 = 55$  Hz,  $F_2 = 165$  Hz.  
Frequency jump when  
 $F_0 = F_2$   
Note also the subharmonic  
regimes

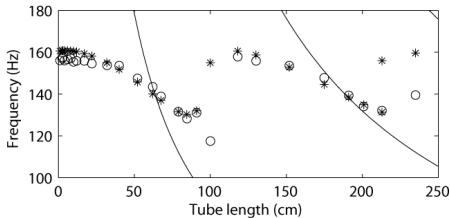
# Phonation threshold pressure



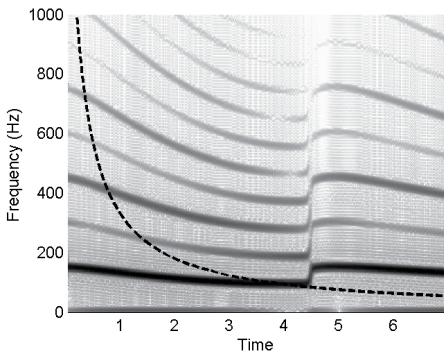
Circles: data from a mechanical replica (Ruty et al., 2008)

Stars: theoretical results

Curves:  $F_1$  and  $F_2$



## Tube of increasing length



Curve:  $F_1$   
Frequency jump when  
 $F_0 \approx F_1$ .

## Source-vocal tract interaction

- Frequency jumps and other sound instabilities may occur when the fundamental frequency of the oscillation crosses a the vocal tract resonances.
- They also require a strong source-vocal tract coupling: large subglottal pressure or small the vocal tract (epilarynx) area.

## Part II

### Articulator kinematics

# Introduction

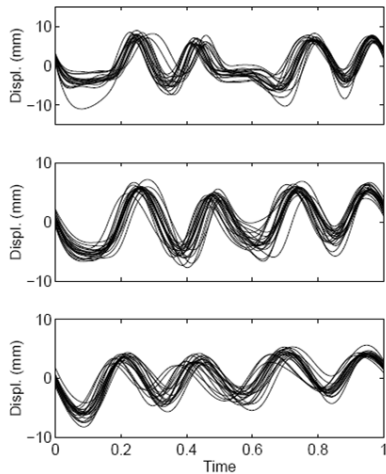
## Question

*Given a set of movement records from a repeated task, how do we determine the common pattern and variations relative to that pattern?*

## Collaborations

- Laura L. Koenig, Haskins Labs and Long Island University
- Anders Löfqvist, Haskins Labs
- Peter Howell, University College London
- Kevin G. Munhall, Queen's University
- Vincent L. Gracco, McGill University

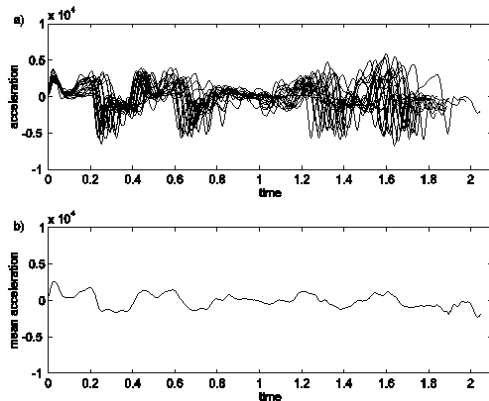
## Example: Lip movements



“Buy Bobby a puppy”, vertical displacement of lower lip (Lucero et al., 1997).

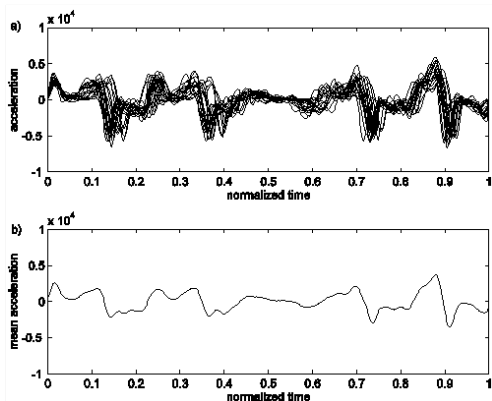
Figure 2: Sets of records at different speaking rates. Top: slow rate. Middle: normal rate. Bottom: fast rate.

## Unnormalized averaging



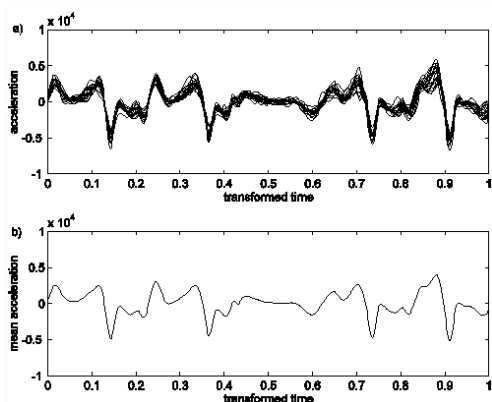
“Buy Bobby a puppy”, vertical acceleration of lower lip.

## Linearly normalized averaging



“Buy Bobby a puppy”, vertical acceleration of lower lip.

## Nonlinearly normalized averaging



“Buy Bobby a puppy”, vertical acceleration of lower lip.

# Functional Data Analysis

- Set of analytical (computationally intensive) tools to explore patterns and variability in sets of data obtained from observations of a repeated physical process (Ramsay and Silverman, 1997).
- Data is recorded discretely, however, FDA assumes that such data may be described by smooth functions of time which may be evaluated at any particular instant of time.
- The main advantage of this approach is that it takes account of the underlying continuity of the physiological system generating the data, and thus it may capture temporal relations in the data owing to this continuity.
- First applied to speech analysis by Ramsay et al. in 1996.
- Matlab Toolbox and other tools:  
<http://ego.psych.mcgill.ca/misc/fda/>

## Functional data

- $N$  records, each record is a set of recorded data  $(t_j, z_j)$ ,  $j = 1, \dots, M$ .
- Assume the existence of a smooth function  $x(t)$  so that  $z_j = x(t_j) + \epsilon_j$ .
- $x(t)$  may be computed at arbitrary  $t$  using smoothing and interpolation techniques.
- Typically, each functional data  $x(t)$  is expressed in terms of a base expansion

$$x(t) = \sum_{k=1}^K c_k \phi_k(t),$$

where  $\phi_k(t)$  could be, e.g., B-splines, triangular functions, exponentials, polynomials, trigonometric functions, etc.

- The smaller  $K$ , the smoother  $x(t)$ .

## Time warping

- Functional data: curves  $x_i(t)$ ,  $i = 1, \dots, N$ .
- For each curve, a transformation of time (warping function) is sought  $h_i(t)$  such that the normalized curves  $x_i^*(t) = x_i[h_i(t)]$  are aligned, according to some measure.
- $h_i(t)$  must be strictly increasing and smooth.
- An auxiliary function  $w_i(t)$  (relative curvature of  $h_i(t)$ ) is defined by

$$\frac{d^2 h_i(t)}{dt^2} = w_i(t) \frac{dh_i(t)}{dt}$$

whose solution is

$$h_i(t) = C_0 + C_1 \int_0^t \exp \left[ \int_0^u w_i(v) dv \right] du$$

- For any continuous  $w_i(t)$ , the above produces  $h_i(t)$  strictly increasing and smooth.
- $w_i(t)$  is the relative curvature of  $h_i(t)$ .

## Measures of alignment

- The algorithm minimizes

$$F_\lambda(h) = \sum_{i=1}^N \int_0^T \{[x_i^*(t) - \bar{x}^*(t)]\}^2 dt + \lambda \int_0^T [w_i(t)]^2 dt$$

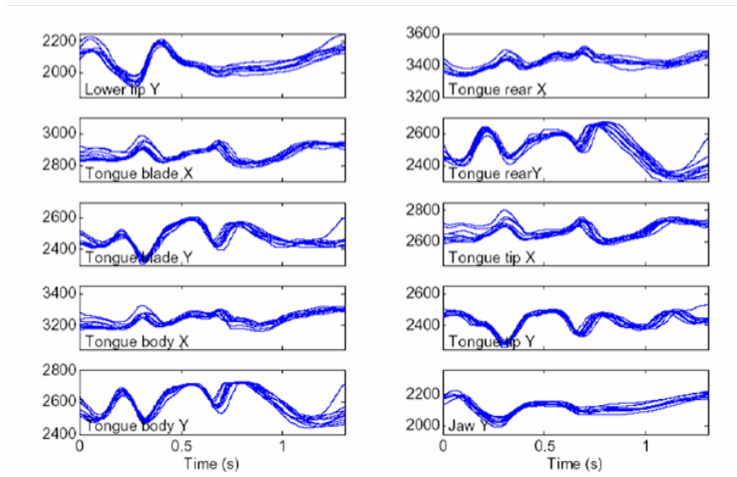
where  $\lambda$  is the roughness penalty coefficient.

- The larger  $\lambda$ , the smoother  $h_i(t)$ . When  $\lambda$  is very large,  $w_i(t) \approx 0$  and  $h_i(t) \approx t$ .
- Even better: instead of the first integral, use the smallest eigenvalue of

$$A = \begin{bmatrix} \int_0^T [\bar{x}^*(t)]^2 dt & \int_0^T x_i^*(t) \bar{x}^*(t) dt \\ \int_0^T x_i^*(t) \bar{x}^*(t) dt & \int_0^T [x_i^*(t)]^2 dt \end{bmatrix}$$

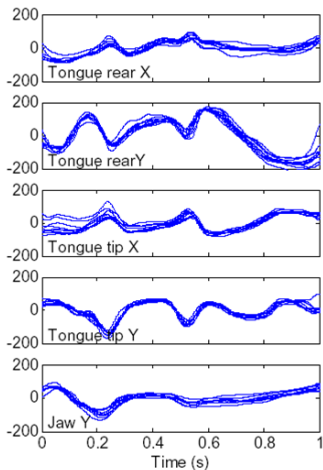
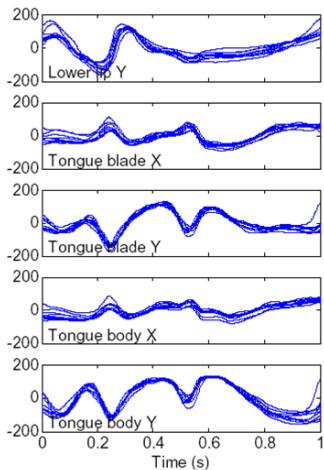
If  $x_i^*(t)$  and  $\bar{x}^*(t)$  differ only by a scale factor (i.e., they have the same shape), then  $A$  is singular and one eigenvalue is zero.

## Example: Multidimensional records



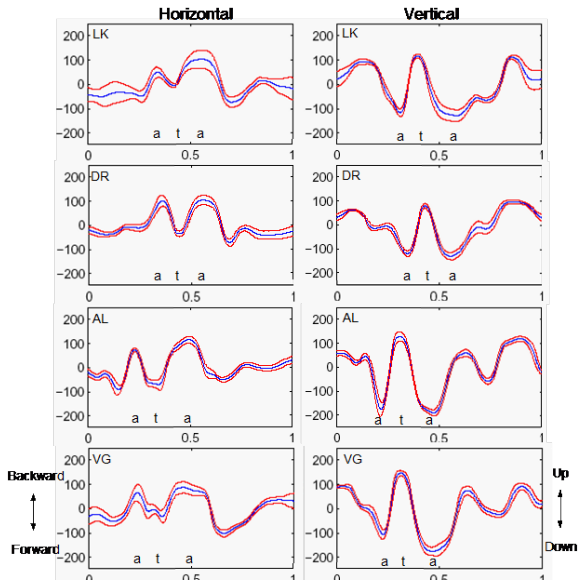
“Say api again”, recorded with magnetometer at Haskins (Lucero and Lofqvist, 2002).

## Example: Multidimensional records



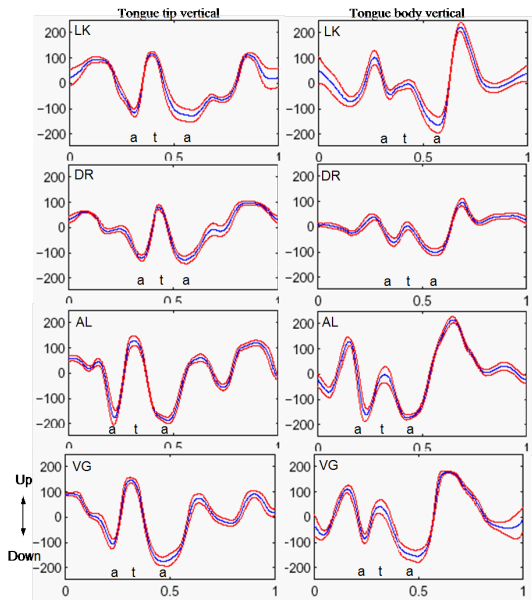
“Say api again”, aligned.

## Results



"Say ata again". Mean  $\pm$  StD for tongue tip movements.

## Results

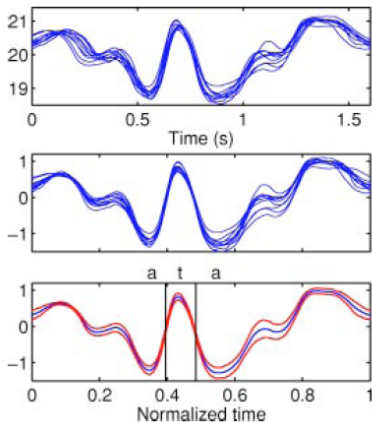


“Say ata again”. Mean  $\pm$  StD for vertical tongue tip and tongue body movements.

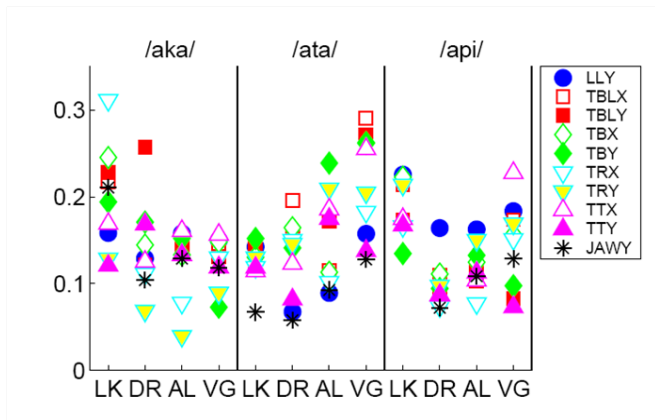
## Variability indices

$$\text{Ampl. var.} = \text{Mean}\{\text{StD}[x_i^*(t)]\}$$

$$\text{Phase var.} = \text{Mean}\{\text{StD}[h_i(t)]\}$$



## Variability indices



(Lucero and Löfqvist, 2005)

## Mathematical model

Clock which produces a certain pattern  $p(t)$  at each cycle, with variations in amplitude and phase (or velocity)

$$x_i(t) = p[t + \phi_i(t)] + \beta_i(t)$$

(Lucero, 2005). Letting  $\theta_i(t) = t + \phi_i(t)$ , then the clock speed (speaking rate) is  $d\theta_i/dt = 1 + d\phi_i/dt$ .

Figure 1. Pattern  $p(\theta)$  used to generate speech trajectories.

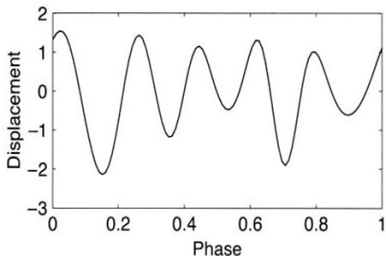
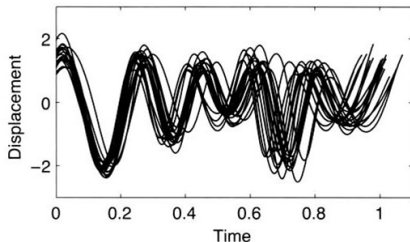


Figure 2. Trajectories for  $k_{\beta} = 0.2$  and  $k_{\gamma} = 0.1$  ( $k_{\beta}$  is the standard deviation of the amplitude variability, and  $k_{\gamma}$  is the standard deviation of the clock's speed variability).



## Time warping, again

- We want to compute a function  $h_i(t)$  such that  $h_i^{-1} = \theta_i(t) = t + \phi_i(t)$ .

- Then

$$x_i[h_i(t)] = x_i^*(t) = p(t) + \beta_i^*(t)$$

and we remove the phase variability.

- $p(t) = \text{Mean } x_i^*(t)$  (assuming  $\text{Mean } \beta_i^*(t) = 0$ )
- $\beta_i^*(t) = p(t) - x_i^*(t)$ .
- $\phi_i[h_i(t)] = \phi_i^*(t) = t - h_i(t)$  is the phase shift or time shift of each point in pattern  $p(t)$ .
- StD  $\phi_i^*(t)$  and StD  $\beta_i^*(t)$  measure the levels of phase and amplitude variability, respectively.

## Variability indices

**Figure 4.** Indices of variability versus  $k_\beta$ , for  $k_\gamma = 0.1$  (constant). (a) Index of amplitude variability and (b) index of phase variability. Circles: actual values; triangles: computed values with unnormalized trajectories; crosses: computed values with linear normalization; stars: computed values with piecewise linearly normalized trajectories; squares: computed values with nonlinearly normalized trajectories.

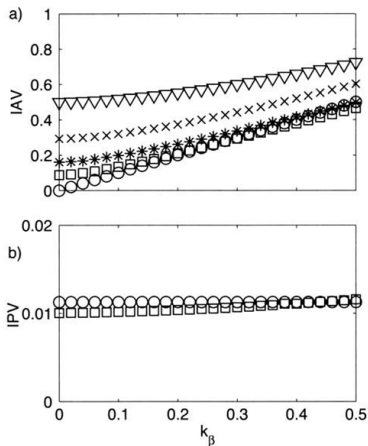
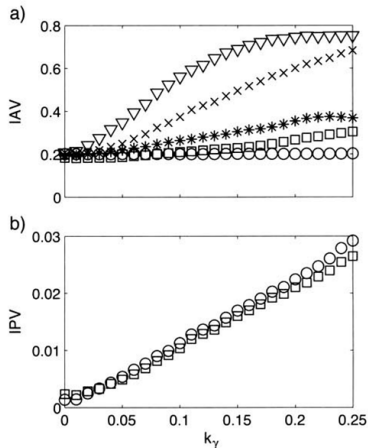


**Figure 5.** Indices of variability versus  $k_\gamma$ , for  $k_\beta = 0.2$  (constant). (a) Index of amplitude variability and (b) index of phase variability. Circles: actual values; triangles: computed values with unnormalized trajectories; crosses: computed values with linear normalization; stars: computed values with piecewise linearly normalized trajectories; squares: computed values with nonlinearly normalized trajectories.



## Part III

# Facial modeling and animation

# Introduction

## Goal

To develop a data-driven facial animation system that could be used as a computational tool in speech production and perception studies. The system must be capable of producing computer-generated animations of speech with an acceptable level of realism, and should allow for direct manipulation of facial movement parameters.

## Applications

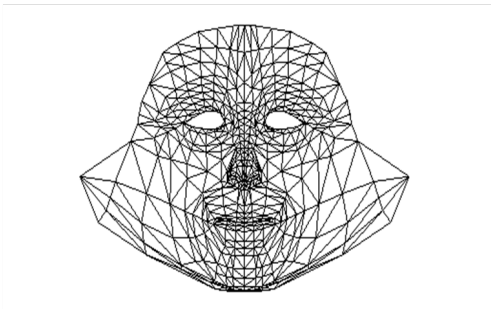
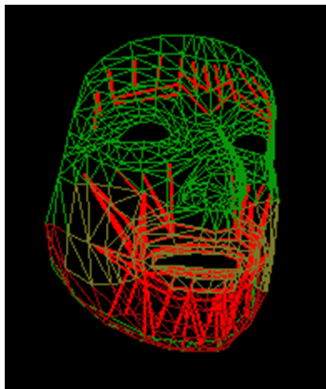
- Understand speech motor control
- Produce realistic facial animation. We seek linguistic realism rather than cosmetic realism.
- Stimulus generation for audiovisual speech research.

## Collaboration

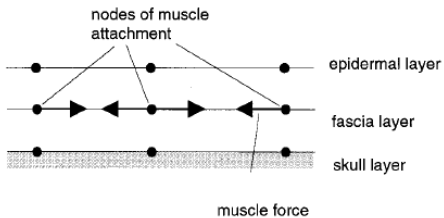
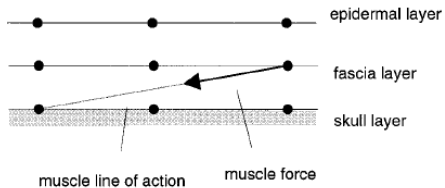
Kevin Munhall, Queen's University

## Theoretical modeling

Based on a a multilayered deformable mesh (Terzopoulos and Waters, 1990)



# Muscle forces



## Mesh equations

For each mesh node  $i$  (512 nodes/layer):

$$m\ddot{\mathbf{x}}_i + r \sum_j (\dot{\mathbf{x}}_i - \dot{\mathbf{x}}_j) + \sum_j \mathbf{g}_{ij} + \sum_e \mathbf{q}_i^e + \mathbf{s}_i + \mathbf{h}_i = \mathbf{F}_i$$

where

$\mathbf{g}_{ij}$ : elastic force (biphasic),

$\mathbf{q}_i$ : incompressibility of skin (volume preservation),

$\mathbf{s}_i$ : force to penalize penetration in the skull,

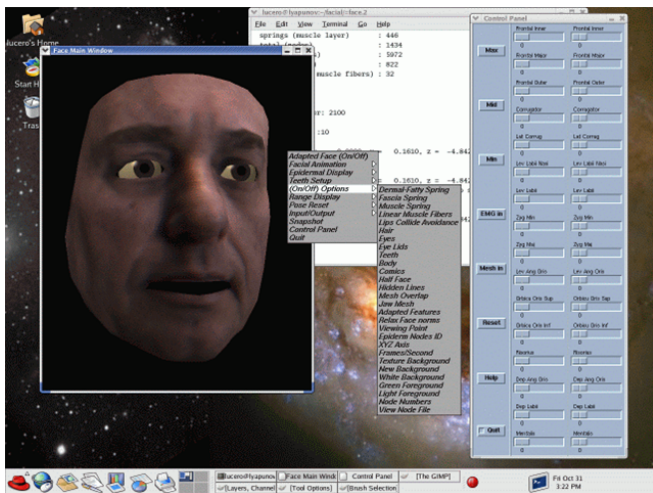
$\mathbf{h}_i$ : tissue connection to the skull,

$\mathbf{F}_i$ : total muscle force.

## Muscle model

- Steady force:  $\bar{M} = k_f SE$ , where  $E$  is the muscle activity
- Graded force development:  $\tau^2 \ddot{M} + 2\tau \dot{M} + M = \bar{M}$  (Laboissière et al., 1996).
- Force-length characteristic:  
 $M^* = M \exp(-|((L/L_0)^{2.3} - 1)/1.26|^{1.62})$  (Brown et al., 1996).
- Force -velocity and passive stiffness characteristics:  
 $F = M^*(f_1 + f_2 + \arctan(f_3 + f_4 \dot{L})) + (k_m \Delta L)^+$  (Laboissière et al., 1996).

# Full model



## Animation

Subject producing /upa/, with a  
bite block to immobilize de jaw.

(Lucero and Munhall, 1999)



## Good, however...

- Intramuscular EMG recording required by the model is an invasive technique with a complex experimental setup.
- The collected signals are still not a good representation of the true muscle activation patterns, due to interdigitation of different muscle fibers, nonlinear transfer functions between EMG and generated force, etc.
- Difficulty of producing a good representation of the facial muscle structure and skin biomechanics that could be adapted to individual speakers

# Empirical modeling

*Given a set of facial movement data during speech, what can we infer about the underlying physiological structure?*

## Assumptions

- The activation of individual muscles produces regional patterns of deformation.
- Such patterns are stable during speech, and occur in small (finite) number.
- The total facial motion is the linear combination of those patterns.

## Approaches

- Kuratate et al (1998), etc.: Principal Component Analysis (PCA) is used to decompose a set of facial shapes into orthogonal components and build a reduced basis of eigenfaces.

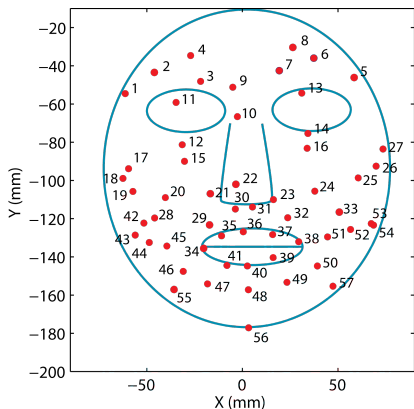
*We want our the model to be expressed in terms of a few facial markers, rather than principal components which have non-trivial physical interpretation.*

- Badin et al (2002), etc.: PCA is used to determine articulatory parameters to control the shape of a 3D vocal tract and face model. Some of the parameters (e.g., jaw height, lip protrusion, etc.) are defined *a priori*, and their contributions are subtracted from the data before computing the remaining components.

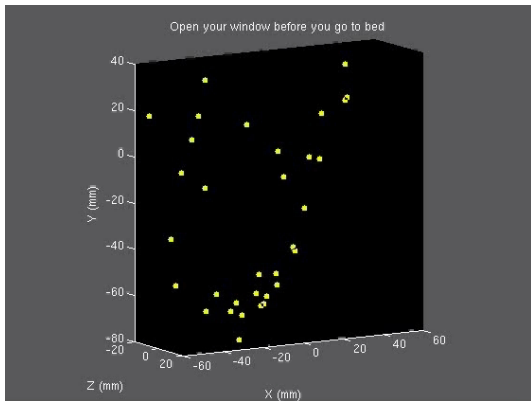
*We want to rely entirely on the data for building the model, with as few prior assumptions as possible.*

## Data

- 3D position of 57 markers on a subject's face, recorded with a Vicon equipment at a 120 Hz sampling frequency, and transformed to head coordinates.
- The subject was producing 40 CID Everyday sentences.
- The subject adopted a consistent rest ("neutral") position at the beginning of each sentence.



## Data example



## Data matrix

$$A = \begin{bmatrix} x_1(t_1) & x_2(t_1) & x_3(t_1) & \cdots & x_n(t_1) \\ x_1(t_2) & x_2(t_2) & x_3(t_2) & \cdots & x_n(t_2) \\ \vdots & \vdots & \vdots & & \vdots \\ x_1(t_m) & x_2(t_m) & x_3(t_m) & \cdots & x_n(t_m) \\ y_1(t_1) & y_2(t_1) & y_3(t_1) & \cdots & y_n(t_1) \\ y_1(t_2) & y_2(t_2) & y_3(t_2) & \cdots & y_n(t_2) \\ \vdots & \vdots & \vdots & & \vdots \\ y_1(t_m) & y_2(t_m) & y_3(t_m) & \cdots & y_n(t_m) \\ z_1(t_1) & z_2(t_1) & z_3(t_1) & \cdots & z_n(t_1) \\ z_1(t_2) & z_2(t_2) & z_3(t_2) & \cdots & z_n(t_2) \\ \vdots & \vdots & \vdots & & \vdots \\ z_1(t_m) & z_2(t_m) & z_3(t_m) & \cdots & z_n(t_m) \end{bmatrix}$$

Which columns (markers) are the most independent?

## QR factorization with column pivoting

- Let  $A$  be an  $m \times n$  data matrix, with  $m \geq n$ . Its QR factorization produces

$$AP = QR$$

where  $P$  is an  $n \times n$  column permutation matrix,  $Q$  is an  $m \times n$  orthogonal matrix, and  $R$  is an  $n \times n$  upper triangular matrix with positive diagonal elements (Golub and Loan, 1996).

- The first column of  $AP$  is the column of  $A$  that has the largest 2-norm.
- The second column of  $AP$  is the column of  $A$  that has the largest orthogonal projection in relation to the first column.
- In general, the  $k$ th column of  $AP$  is the column of  $A$  with the largest orthogonal projection to the first  $k - 1$  columns.
- Diagonal elements of  $R$  ( $R_{k,k}$ , called “ $R$  values”): orthogonal components of each column  $k$  relative to the first  $k - 1$  columns, in decreasing order for  $k = 1, \dots, n$ . They are close to the singular values in the SVD decomposition.
- The first columns of  $AP$  are well conditioned (independent).

## The subset selection problem

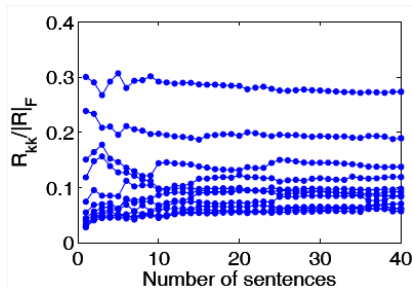
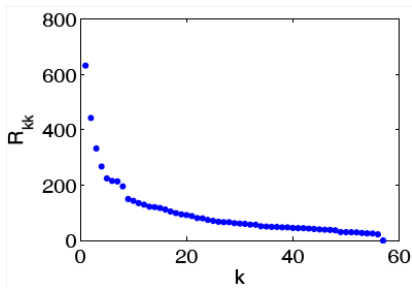
- Given a data matrix  $A$ , and an observation vector  $b$ , find a predictor vector  $x$  in the least squares sense which minimizes  $\|Ax - b\|_2^2$ . However, instead of using the whole data matrix  $A$  to predict  $b$ , use only a subset of its columns (the most non-redundant columns). How to pick those columns?
- Solution: compute  $AP = QR$ . Then select the first  $k$  columns of  $AP$ .
- We may use the  $k$  most independent columns of  $A$ , ( $AP_1$ ) to predict the other (redundant) columns ( $AP_2$ ), in the least squares sense. If

$$R = \begin{bmatrix} R_{11} & R_{12} \\ 0 & R_{22} \end{bmatrix}, \quad P = [P_1 P_2],$$

then the solution of  $R_{11}X = R_{12}$  is a minimizer of

$$E = \|AP_1X - AP_2\|_F^2$$

## R values



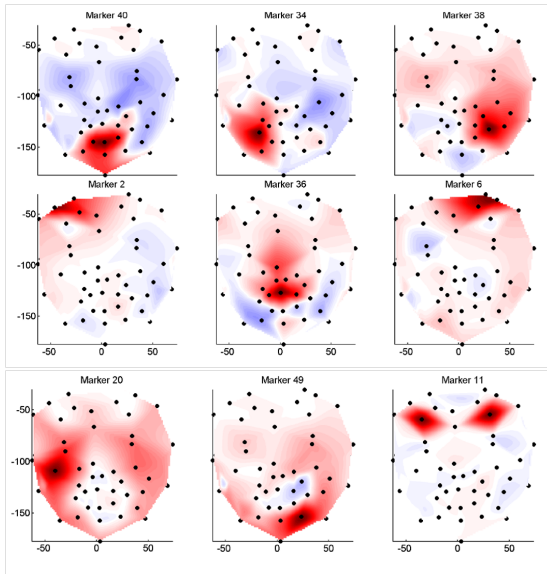
Elements in the main diagonal of  $R$ . Represent the size of the orthogonal components of each column of  $AP$ .

## Most independent markers

- Data sets: 30 sentences, different for each trial.
- First marker: #40 or #48, center of the lower lip or just below.
- Next two markers: #34 and #38, lip corners.
- Fourth marker: #2, center of the left eyebrow.

Order	Trials					...
	1	2	3	4	8	
1	40	40	40	40	48	
2	34	34	34	34	34	
3	38	38	38	38	38	
4	2	2	2	2	2	
5	36	36	36	6	36	
6	6	6	49	36	6	...
7	20	49	20	20	20	
8	49	20	6	49	39	
9	11	11	11	11	49	
10	52	54	52	52	13	
11	54	47	54	54	54	
12	47	23	47	56	52	

## Independent kinematic regions



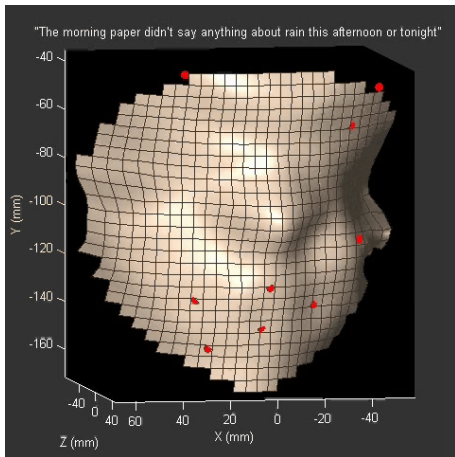
Kinematic regions:  
least square fit of  
remaining markers,  
extended to the whole  
face by cubic  
interpolation.

Red and blue  
subregions: motion in  
the same and  
opposite direction,  
respectively, to the  
main marker's  
motion.

# Computer generation of facial animations

- Facial animations of arbitrary speech utterances may be produced by driving the independent kinematic regions with collected signals.
- The position of other arbitrary facial points may be generated by using, e.g., cubic interpolation
- Using only 9 regions, the animations look visually realistic, without any noticeable distortion in the motion pattern. The error of the reconstructed trajectories of facial markers is low, with mean value around 1 mm.

## Animation example



(Lucero and Munhall, 2008)

## Part IV

### Final remarks

## About models

*Milk production at a dairy farm was low so the farmer wrote to the local university, asking help from academia. A multidisciplinary team of professors was assembled, headed by a theoretical physicist, and two weeks of intensive on-site investigation took place. The scholars then returned to the university, notebooks crammed with data, where the task of writing the report was left to the team leader. Shortly thereafter the farmer received the write-up, and opened it to read on the first line:*

*“Consider a spherical cow in vacuum...”*



(From Wikipedia)

## Acknowledgments

Support by MCT/CNPq and CAPES/MEC (Brazil)

## Contact

lucero@unb.br

<http://www.mat.unb.br/lucero/>